

## ORIGINAL ARTICLE

# Pilot study on evaluation of any correlation between MR perfusion ( $K^{\text{trans}}$ ) and diffusion (apparent diffusion coefficient) parameters in brain tumors at 3 Tesla

Jian-Ping Chu, Henry Ka-Fung Mak, Kelvin Kai-Wing Yau, Linda Zhang, Janice Tsang, Queenie Chan and Gilberto Ka-Kit Leung

*Department of Diagnostic Radiology, University of Hong Kong, Hong Kong, Hong Kong*

*Corresponding address: Dr Henry Ka-Fung Mak, Department of Diagnostic Radiology, University of Hong Kong, Hong Kong, Hong Kong.  
Email: makkf@hkucc.hku.hk*

Date accepted for publication 7 November 2011

### Abstract

**Purpose:** To assess any correlation of volume transfer constant ( $K^{\text{trans}}$ ) with apparent diffusion coefficient (ADC) in different brain tumor types at 3 T magnetic resonance (MR) imaging. **Materials and methods:** Thirteen patients with brain tumors (8 men, 5 women; mean age  $54.6 \pm 17.7$  years) were enrolled in this retrospective study. All patients underwent dynamic contrast-enhanced  $T_1$ -weighted MR perfusion and diffusion-weighted imaging using a 3 T scanner.  $K^{\text{trans}}$  was estimated by specially designed software. For each tumor, regions of interest (ROIs) were manually selected on corresponding  $K^{\text{trans}}$  and ADC maps. Pearson correlation coefficients were obtained for maximum, mean and minimum values of  $K^{\text{trans}}$  and ADC of all ROIs. Based on clinicopathologic results, the final diagnoses of patients were glioblastoma multiforme (3), low-grade to anaplastic gliomas (4), meningiomas (3) and metastatic tumors (3). **Results:**  $K^{\text{trans}}$ (max) values were significantly inversely correlated with ADC(min) values ( $r = -0.536$ ,  $P < 0.001$ ) and ADC(mean) values ( $r = -0.465$ ,  $P < 0.001$ ).  $K^{\text{trans}}$ (mean) and  $K^{\text{trans}}$ (min) values were significantly inversely correlated with ADC(mean) ( $r = -0.228$ ,  $P = 0.038$ ) and ADC(max) values ( $r = -0.355$ ,  $P = 0.001$ ), respectively. **Conclusion:** We found that irrespective of brain tumor type, there is an inverse correlation between ADC and  $K^{\text{trans}}$ . Our findings highlight an intricate relationship between vascular permeability and the tumor microenvironment, probably modulating and/or interacting with changes such as increased cellularity, ischemic insult and varying extracellular matrix composition.

**Keywords:** *Dynamic contrast-enhanced MRI; diffusion-weighted imaging; brain tumor; apparent diffusion coefficient; permeability; blood–brain barrier.*

## Introduction

The World Health Organization grading system of cerebral tumors is based on criteria such as cellular and nuclear pleomorphism, increased cellularity, microvascular proliferation, and/or necrosis. These features tend to appear in a predictable sequence<sup>[1]</sup>. Microvascular proliferation can be assessed by microvessel density in postoperative specimens and vascular endothelial growth factors (VEGF) by serum studies<sup>[2]</sup>. Recent evidence suggests that vascular permeability and the presence of VEGF/vascular permeability factor are important

mediators of brain tumor growth in addition to angiogenesis<sup>[3]</sup>.

Previous studies on perfusion and permeability magnetic resonance imaging (MRI), either by  $T_1$  dynamic contrast-enhanced (DCE MRI or  $T_2^*$  dynamic susceptibility contrast (DSC) MRI, had shown correlations between regional cerebral blood volume, microvascular permeability and tumor grading<sup>[4–7]</sup> as well as molecular markers such as VEGF<sup>[8,9]</sup>. In the last decade, many studies on the measurement of volume transfer constant ( $K^{\text{trans}}$ ) in different types of brain tumors were published<sup>[10–14]</sup>. Despite variations in acquisition methods and

**Table 1** A summary of demographic data, clinical and histological diagnoses of 13 patients

| Age (years) | Gender | Clinical diagnosis                                              | Histologic diagnosis                                       | Use of steroids prior to MRI |
|-------------|--------|-----------------------------------------------------------------|------------------------------------------------------------|------------------------------|
| 27          | M      | Duodenal stromal tumor, left frontal temporal tumor             | Metastatic gastrointestinal stromal tumor                  | Nil                          |
| 30          | M      | Right temporal parietal tumor                                   | Anaplastic oligoastrocytoma, (grade III)                   | Nil                          |
| 41          | M      | Left frontal tumor                                              | Astrocytoma (grade II)                                     | Nil                          |
| 46          | M      | Left frontal tumor                                              | Anaplastic oligoastrocytoma (grade III)                    | No steroids                  |
| 48          | M      | Turcot syndrome, left frontal tumor                             | Oligoastrocytoma (grade II, progressing to grade III)      | Nil                          |
| 48          | F      | Right upper lobe lung mass, left temporal tumor                 | High-grade malignant tumor, consistent with rhabdoid tumor | Steroids for 1 day           |
| 51          | M      | Splenium of corpus callosum                                     | Glioblastoma in background of gemistocytic astrocytoma     | Nil                          |
| 55          | M      | Left insula tumor                                               | Glioblastoma                                               | Nil                          |
| 57          | F      | Known parasagittal meningioma                                   | Nil                                                        | Nil                          |
| 72          | F      | Solitary right inferior parietal tumor, known carcinoma of lung | Nil                                                        | Nil                          |
| 74          | F      | Known frontal meningioma                                        | Nil                                                        | Nil                          |
| 77          | M      | Left temporal tumor                                             | GBM                                                        | No record available          |
| 84          | F      | Left parietal tumor                                             | Meningioma                                                 | Steroid for 1 day            |

pharmacokinetic modeling (either first-pass T2\* DSC MRI or steady-state T1 DCE MRI), these studies have validated the consistencies in the quantitative measurement of  $K^{\text{trans}}$  and other kinetic parameters such as total extravascular extracellular space (EES) ( $v_e$ )<sup>[15]</sup>.

Another key histologic feature in tumor grading is cellular density. Diffusion-weighted imaging (DWI) has been successful in assessing cellularity of brain tumors as apparent diffusion coefficient (ADC) is thought to be inversely correlated with tumor cellularity and hence glioma grade<sup>[16,17]</sup>. A recent study by Murakami et al.<sup>[18]</sup> found that combining ADC difference values with minimum values facilitated grading of astrocytic tumors despite background heterogeneity. The role of DWI in other tumor types has also been explored<sup>[19,20]</sup>. Generally speaking, ADC is not sensitive enough to differentiate between different tumor pathologies. Nonetheless, ADC has been proposed as an early biomarker for tumor response<sup>[21]</sup>. An increase in ADC was found to occur shortly after successful treatment, which correlated with breakdown of cellular membranes and reduction in cell density, both preceding changes in tumor size.

Although ADC is thought to be inversely correlated with tumor cellularity, a recent study on oligodendrogliomas showed no such relationship<sup>[22]</sup>. The complex nature of the tumor microenvironment is further exemplified by a recent study that found no relationship between  $v_e$  and ADC<sup>[23]</sup>, although both parameters are postulated to be inversely related to cellularity.

As  $K^{\text{trans}}$  (index of endothelial permeability) and ADC (marker of tissue water diffusion restriction and cellularity) provide physiologic and functional information on

the tumor microenvironment, we hypothesize that there exists an intricate relationship between them. In addition, we attempt to explore this relationship in a wide spectrum of brain tumors, which we found lacking in the current literature because previous studies tend to focus on a single type of brain pathology. In this pilot study, we attempt to evaluate the correlation between  $K^{\text{trans}}$  and ADC in different types of brain tumors at 3 T MRI and the possible underlying mechanisms.

## Materials and methods

### Patients

All patients were scanned either for preoperative assessment or clinical management, with informed consent obtained for use of their MR images. Local institutional review board approval was not required for such a retrospective study.

Thirteen patients with different types of brain tumor (8 male and 5 female patients; mean age 54.6 years  $SD \pm 17.7$  years) were enrolled in this retrospective study between August 2009 and March 2010. All patients underwent preoperative T1 DCE MR perfusion and DWI using a 3 T MRI scanner.

In 10 of the 13 patients, pathologic results were obtained either postoperatively or at biopsy and for the remaining 3 patients, clinical diagnoses were based on medical history and brain MRI. They were classified into 4 groups (Table 1): (1) glioblastoma multiforme (GBM) (3 cases); (2) astrocytoma/oligoastrocytoma/anaplastic oligoastrocytoma (4 cases); (3) meningioma (3 cases); (4) metastatic carcinoma (3 cases).

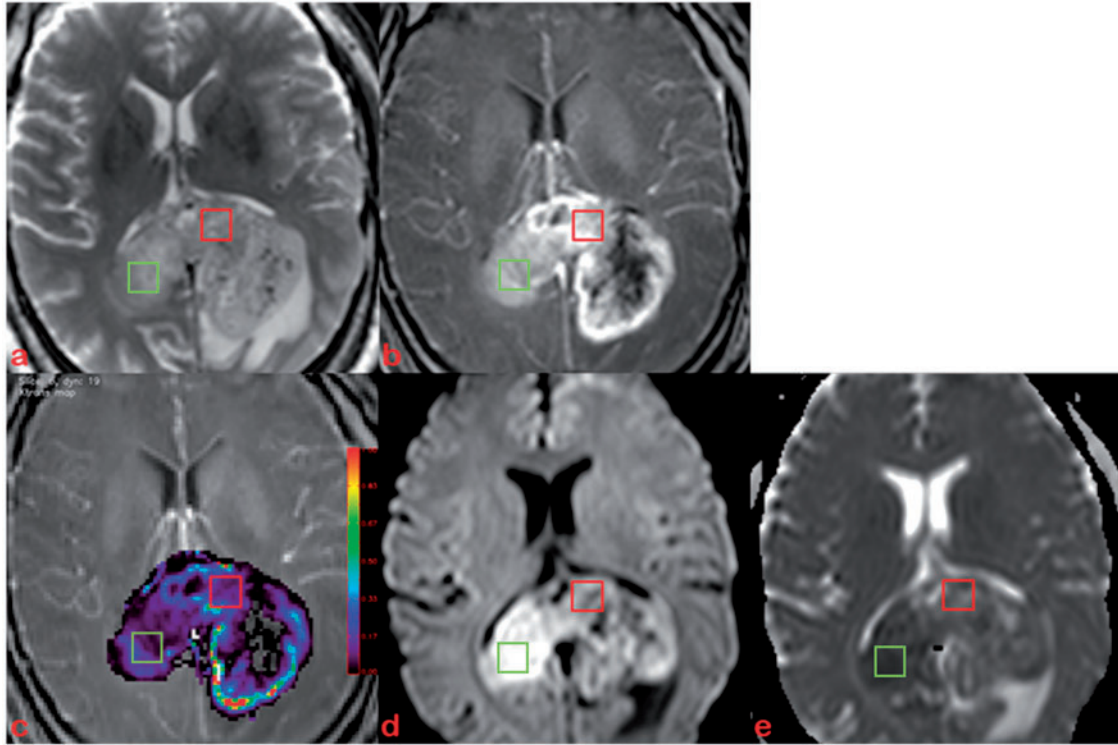


**Figure 1** Axial T<sub>2</sub>-weighted image (a), post-contrast T<sub>1</sub>-weighted image (b) of a 51-year-old man with GBM in splenium of corpus callosum. Five to 7 ROIs (40–60 mm<sup>2</sup>, 2 examples shown) were manually selected on the corresponding slices of K<sup>trans</sup> (c), DWI (d) and ADC map (e) using Image J.

### Imaging protocol

All MRI studies were performed with a 3 T MRI scanner (Philips Healthcare, Netherlands). Conventional MRI, DCE images and DWI were acquired during the same procedure. Conventional MRI consisted of a T<sub>1</sub>-weighted sequence (inversion recovery turbo spin-echo, repetition time (TR)/time for inversion (TI) 2000/800 ms, echo time (TE) 20 ms, field of view (FOV) 230 × 230 × 137 mm, slice thickness 5 mm, gap 0.5 mm); T<sub>2</sub>-weighted sequence (spin-echo, TR/TE 3937/80 ms, FOV 230 × 230 × 137 mm, slice thickness 5 mm, gap 0.5 mm); susceptibility weighted imaging (three-dimensional (3D) T<sub>1</sub>-weighted fast-field echo (FFE), TR/TE 17/24 ms, flip angle 15°, voxel size 0.9 × 0.9 × 2 mm<sup>3</sup>); fluid attenuated inversion recovery (TR/TI 11000/2800 ms, TE 125 ms, slice thickness 5 mm, gap 0.5 mm, coronal plane).

DWIs were acquired in the transverse plane by using a spin-echo single-shot echoplanar imaging sequence (TR/TE 3491/44 ms, FOV 230 × 230 × 137 mm, thickness 5 mm, flip angle 90°, b-values of 0 and 1200 s/mm<sup>2</sup>).

Pre-contrast 3D FFE images were acquired prior to contrast injection (TR/TE 13/1.36 ms, FOV 230 × 193 × 70 mm, voxel size 1.4 × 1.4 × 6 mm<sup>3</sup>, flip angle 5°). This was followed by a DCE series using the same sequence except for a flip angle of 15°. After 10 dynamic scans, a bolus of 0.1 mmol/kg gadoteric acid

(Dotarem; Guerbet, France) was injected intravenously at 3 ml/s, followed by saline flush of an equal amount. Conventional contrast-enhanced T<sub>1</sub>-weighted sequence (spin-echo, TR/TE 450/10 ms, FOV 230 × 230 × 137 mm; slice thickness 5 mm, gap 0.5 mm) was also obtained afterwards.

### Image processing

K<sup>trans</sup> was estimated by specially designed software<sup>[24]</sup> based on the two-compartment model (generalized kinetic model), which has been described thoroughly in a previous review by Tofts et al.<sup>[25]</sup>. K<sup>trans</sup>, one of the principle parameters, is equal to the product of the capillary wall permeability and capillary wall surface area per unit volume. K<sup>trans</sup> maps were automatically generated by this software, after input of preliminarily acquired T<sub>1</sub>-weighted maps of flip angle 5° and 15°. In this procedure, the anterior cerebral artery (ACA) was selected as arterial input function (AIF). K<sup>trans</sup> and ADC maps were then quantitatively analyzed using Image J software. For each tumor, 5 to 7 ROIs of 40–60 mm<sup>2</sup> were manually selected on the corresponding slices of K<sup>trans</sup> and ADC maps (Fig. 1) by an experienced radiologist (JPC), supervised by a neuroradiologist (HKM). Both had more than 10 years experience in reading brain images. ROI selection was based on enhanced T<sub>1</sub>-weighted images avoiding

necrotic and cystic components. For low-grade gliomas, T<sub>1</sub>-weighted and T<sub>2</sub>-weighted images were also used in addition to enhanced T<sub>1</sub>-weighted images for ROI placement. The maximum, mean and minimum values of K<sup>trans</sup> and ADC in each ROI were calculated by Image J. There were 83 ROIs in total: group 1 (20), group 2 (24), group 3 (20) and group 4 (19).

### Statistical analysis

The mean  $\pm$  SD of maximum, mean and minimum values of K<sup>trans</sup> and ADC in all ROIs were computed. Correlation between these values of K<sup>trans</sup> and ADC were analyzed by Pearson correlation.

## Results

### Correlation of K<sup>trans</sup> and ADC values

The mean  $\pm$  SD of maximum, mean and minimum values of K<sup>trans</sup> and ADC for 83 ROIs are summarized in Table 2.

K<sup>trans</sup>(max) values were significantly inversely correlated with ADC(min) values ( $r = -0.536$ ,  $P < 0.001$ ) and ADC(mean) values ( $r = -0.465$ ,  $P < 0.001$ ); K<sup>trans</sup>(mean) values were also inversely correlated with ADC(mean) ( $r = -0.228$ ,  $P = 0.038$ ) and ADC(max) ( $r = -0.421$ ,  $P < 0.001$ ) values; K<sup>trans</sup>(min) values were significantly inversely correlated with ADC(max) values ( $r = -0.355$ ,  $P = 0.001$ ) and significantly directly correlated with ADC(min) values ( $r = 0.222$ ,  $P = 0.043$ ) (Table 3).

**Table 2** The mean  $\pm$  SD of maximum, mean and minimum values of K<sup>trans</sup> and ADC in 83 ROIs

|                           | Mean $\pm$ SD   |
|---------------------------|-----------------|
| K <sup>trans</sup> (mean) | 0.34 $\pm$ 0.27 |
| K <sup>trans</sup> (min)  | 0.21 $\pm$ 0.20 |
| K <sup>trans</sup> (max)  | 0.91 $\pm$ 1.01 |
| ADC (mean)                | 0.90 $\pm$ 0.30 |
| ADC (min)                 | 0.73 $\pm$ 0.26 |
| ADC (max)                 | 1.16 $\pm$ 0.41 |

K<sup>trans</sup> measurements are expressed/min; ADC measurements are expressed in  $\times 10^{-3}$  mm<sup>2</sup>/s.

**Table 3** The correlation between K<sup>trans</sup> and ADC in all ROIs ( $n = 83$ )

|              |                     | ADC(mean) | ADC(min) | ADC(max) |
|--------------|---------------------|-----------|----------|----------|
| Ktrans(mean) | Pearson correlation | -0.228*   | -0.004   | -0.421** |
|              | (P value)           | (0.038)   | (0.968)  | (<0.001) |
| Ktrans(min)  | Pearson correlation | -0.033    | 0.222*   | -0.355** |
|              | (P value)           | (0.770)   | (0.043)  | (0.001)  |
| Ktrans(max)  | Pearson correlation | -0.465**  | -0.536** | -0.097   |
|              | (P value)           | (<0.001)  | (<0.001) | (0.383)  |

\*Correlation is significant at a 0.05 significance level (2-tailed).

\*\*Correlation is significant at a 0.01 significance level (2-tailed).

## Discussion

Our results demonstrated that irrespective of tumor type, K<sup>trans</sup>(max) values were significantly inversely correlated with ADC(min) values ( $r = -0.536$ ,  $P < 0.001$ ), and K<sup>trans</sup>(mean) values were significantly inversely correlated with ADC(mean) ( $r = -0.228$ ,  $P = 0.038$ ).

To our knowledge, this relationship has not been reported in a single study based on a spectrum of brain tumor types. The findings supported our hypothesis that there was an intricate relationship between capillary membrane permeability and water diffusion property in the tumor microenvironment although the exact mechanism is not understood. A similar observation had been reported by Langer et al.<sup>[26]</sup> in prostate cancer although the inverse correlation between K<sup>trans</sup> and ADC was weak in their study (Pearson correlation coefficient = -0.213).

We propose several possibilities for this phenomenon in our study. First, this significant inverse correlation between K<sup>trans</sup>(max) and ADC(min) or K<sup>trans</sup>(mean) and ADC(mean), irrespective of tumor type, might be explained by tumor cellularity. Yankeelov et al.<sup>[27]</sup> found that lower ADC values correspond to increased K<sup>trans</sup> in pre-treatment breast cancer, and the authors reasonably expected that areas of rapid proliferation and increased cell density present a decreased ADC. Moreover, high-grade tumors with florid microvascular proliferation tend to have an increase in immature tumoral vessels, which might also explain the inverse correlation between K<sup>trans</sup> and ADC<sup>[28]</sup>.

However, a word of caution should be made prior to this generalization. Theoretical Monte Carlo simulations suggest that changes in tissue water diffusion following tissue damage are predominately attributable to alterations in the volume and tortuosity of the extracellular space. Although these properties of the extracellular space are primarily a function of cell density, ADC values cannot predict tumor cellularity<sup>[29]</sup>.

Second, rapidly growing tumors are capable of outstripping their vascular supply, leading to cellular ischemia. DWI has been shown to be efficacious in demonstrating areas of acute infarction in the setting of brain tumors<sup>[30]</sup>. In a recent study of blood-brain barrier leakage in rats<sup>[31]</sup> following temporary focal cerebral

ischemia, ADC values were significantly inversely correlated and ischemic lesion volumes significantly directly correlated with  $K^{\text{trans}}$  values. The results further showed that after ischemia reperfusion in rats, the magnitude of blood–brain barrier leakage diminished over time and correlated with the severity and extent of ischemic injury. Hence, besides increased cellularity, ischemic episodes in tumors might be partly responsible for our findings.

Third, extracellular matrix composition might be an additional factor. Jenkinson *et al.*<sup>[22]</sup> found no linear correlation between mean ADC and mean cell density in oligodendroglial tumors and suggested that the composition of the extracellular matrix might influence ADC more than cellularity. Hyaluronan, one of the main hydrophilic components of the extracellular matrix in gliomas, contributing to ADC differences between high- and low-grade glial tumors has been proposed<sup>[32]</sup>.

Moreover, interstitial edema might affect the extracellular composition in tumors with a leaky blood–brain barrier. The study of therapeutic response in breast carcinoma by Yankeelov *et al.*<sup>[27]</sup> reported a negative correlation between  $v_e$  and ADC values, with ADC increasing and  $v_e$  decreasing following treatment. They hypothesized that these findings may reflect a decrease in interstitial fluid pressure following treatment, aiding the elimination of cell debris and causing an increase in ADC but an overall decrease in  $v_e$ . In the study by Mills *et al.*<sup>[23]</sup>, the authors hypothesized that both ADC and  $v_e$  reflect the size of the EES in patients with GBM but found no direct correlation between the 2 parameters. Their findings revealed the complex nature of the tumor environment and supported our views that ADC may be influenced by multiple parameters, some of which are proposed in the current study.

The limitations of our study were as follows: first, the relatively small sample size (83 ROI records from 13 patients). Hence, our findings should be further evaluated and confirmed by a large-scale study. Second, the choice of ACA for AIF was empirical. It was based on a subgroup analysis of our dataset (8 patients) using either anterior cerebral, right middle cerebral or left middle cerebral arteries as AIF, which revealed that ACA as input resulted in the best shape of the AIF curve. Although ACA as AIF input also led to higher absolute  $K^{\text{trans}}$  values compared with the other 2, our observations based on statistical trends were unlikely to be affected. Furthermore, the cranio-caudal coverage was limited (only 7 cm) in the DCE study and could not include the proximal middle cerebral arteries in some patients. Conversely, the anterior cerebral arteries could be consistently located for all patients. Third, any use of steroids could affect ADC and  $K^{\text{trans}}$  results. In our study, 10 of 13 patients did not receive any steroids prior to MRI scanning and 2 were on steroids for just 1 day (Table 1). The effect of steroids in our group of patients was therefore minimal.

## Conclusion

We found that irrespective of brain tumor type, there is an inverse relationship between ADC and  $K^{\text{trans}}$ . Our finding highlights an intricate relationship between vascular permeability and the tumor microenvironment, probably modulating and/or interacting with changes such as increased cellularity, ischemic insult and varying extracellular matrix composition.

## Acknowledgment

We would like to thank Arjan W Simonetti (Philips Healthcare, Netherlands), for use of software for  $K^{\text{trans}}$  measurements and the technical staff of the 3 T MRI unit (especially Mr Ken Liu), University of Hong Kong, for their uncompromising support.

## References

- [1] Louis DN, Ohgaki H, Wiestler OD, *et al.* The 2007 WHO classification of tumors of the central nervous system. *Acta Neuropathol* 2007; 14: 97–109.
- [2] Vermeulen PB, Gasparini G, Fox SB, *et al.* Quantification of angiogenesis in solid human tumors: an international consensus on the methodology and criteria of evaluation. *Eur J Cancer* 1996; 32A: 2474–84.
- [3] Lacerda S, Law M. Magnetic resonance perfusion and permeability imaging in brain tumors. *Neuroimaging Clin North Am* 2009; 19: 527–57. doi:10.1016/j.nic.2009.08.007.
- [4] Roberts HC, Roberts TP, Brasch RC, Dillon WP. Quantitative measurement of microvascular permeability in human brain tumors achieved using dynamic contrast-enhanced MR imaging: correlation with histologic grade. *AJNR Am J Neuroradiol* 2000; 21: 891–9.
- [5] Provenzale JM, Wang GR, Brenner T, Petrella JR, Sorensen AG. Comparison of permeability in high grade and low grade brain tumors using dynamic susceptibility contrast MR imaging. *AJR Am J Roentgenol* 2002; 178: 711–16.
- [6] Law M, Yang S, Babb JS, *et al.* Comparison of cerebral blood volume and vascular permeability from dynamic susceptibility contrast-enhanced perfusion MR imaging with the glioma grade. *AJNR Am J Neuroradiol* 2004; 25: 746–55.
- [7] Yang S, Law M, Babb JS, *et al.* Dynamic contrast enhanced with perfusion MRI imaging measurements of endothelial permeability: differentiation between atypical and typical meningiomas. *AJNR Am J Neuroradiol* 2003; 24: 1554–9.
- [8] Haris M, Husain N, Singh A, *et al.* Dynamic contrast enhanced derived cerebral blood volume correlates better with leak correction than with no correction for vascular endothelial growth factor, microvascular density, and grading of astrocytoma. *J Comput Assist Tomogr* 2008; 32: 955–65. doi:10.1097/RCT.0b013e31816200d1.
- [9] Maia AC, Jr. Malheiros SM, da Rocha AJ, *et al.* MR cerebral blood volume maps correlated with vascular endothelial growth factor expression and tumor grade in nonenhancing gliomas. *AJNR Am J Neuroradiol* 2005; 26: 777–83.
- [10] Zhu XP, Li KL, Kamaly-Asl ID, *et al.* Quantification of endothelial permeability, leakage space, and blood volume in brain tumors using combine that T1 and T2\* contrast enhanced dynamic MR imaging. *J Magn Reson Imaging* 2000; 11: 575–85. doi:10.1002/1522-2586(200006)11:6<575::AID-JMRI2>3.0.CO;2-1.
- [11] Johnson G, Wetzel SG, Cha S, Babb J, Tofts PS. Measuring blood volume and vascular transfer of constant from dynamic,

- T2\*-weighted contrast-enhanced MRI. *Magn Reson Med* 2004; 51: 961–8. doi:10.1002/mrm.20049.
- [12] Haroon HA, Buckley DL, Patankar TA, et al. A comparison of  $k^{\text{trans}}$  measurements obtained with conventional and first-pass pharmacokinetic models in human gliomas. *J Magn Reson Imaging* 2004; 19: 527–36. doi:10.1002/jmri.20045.
- [13] Cha S, Yang L, Johnson G, et al. Comparison of microvascular permeability measurements,  $k^{\text{trans}}$ , determined with conventional steady-state T1-weighted and first-pass T2\*-weighted MR imaging methods in gliomas and meningiomas. *AJNR Am J Neuroradiol* 2006; 27: 409–17.
- [14] Larsson HBW, Courivaud F, Rostrup E, Hansen AE. Measurement of brain perfusion, blood volume, and blood brain barrier permeability, using dynamic contrast enhanced T1 weighted MRI at 3 tesla. *Magn Reson Med* 2009; 62: 1270–81. doi:10.1002/mrm.22136.
- [15] Zhu XP, Li KL, Jackson A, Buckley DL, Parker GJM, editors. Dynamic contrast-enhanced MRI in cerebral tumors. In: Jackson A, Buckley DL, Parker GJM, editors. Dynamic contrast-enhanced magnetic resonance imaging in oncology. Berlin: Springer; 2005, p. 130.
- [16] Sugahara T, Korogi Y, Kochi M, et al. Usefulness of diffusion-weighted MRI with echo-planar technique in the evaluation of cellularity in gliomas. *J Magn Reson Imaging* 1999; 9: 53–60. doi:10.1002/(SICI)1522-2586(199901)9:1<53::AID-JMRI7>3.0.CO;2-2.
- [17] Guo AC, Cummings TJ, Dash RC, Provenzale JM. Lymphomas and high-grade astrocytomas: comparison of water diffusibility and histologic characteristics. *Radiology* 2002; 224: 177–83. doi:10.1148/radiol.2241010637.
- [18] Murakami R, Hirai T, Sugahara T, et al. Grading astrocytic tumors by using apparent diffusion coefficient parameters. *Radiology* 2009; 251: 838–45. doi:10.1148/radiol.2513080899.
- [19] Kono K, Inoue Y, Nakayama K, et al. The role of diffusion weighted imaging in patients with brain tumors. *AJNR Am J Neuroradiol* 2001; 22: 1081–8.
- [20] Server A, Kulle B, Mahlen J, et al. Quantitative apparent diffusion coefficients in the characterization of brain tumors and associated peritumoral edema. *Acta Radiol* 2009; 6: 682–9.
- [21] Hamstra DA, Rehemtulla A, Ross BD. Diffusion on magnetic resonance imaging: a biomarker for treatment response in oncology. *J Clin Oncol* 2007; 25: 4104–9. doi:10.1200/JCO.2007.11.9610.
- [22] Jenkinson MD, du Plessis DG, Smith TS, Brodbelt AR, Joyce KA, Walker C. Cellularity and apparent diffusion coefficient in oligodendroglial tumors characterized by genotype. *J Neurooncol* 2010; 96: 385–92. doi:10.1007/s11060-009-9970-9.
- [23] Mills SJ, Soh C, Rose CJ, et al. Candidate biomarkers of extravascular extracellular space: a direct comparison of apparent diffusion coefficient and dynamic contrast-enhanced MR imaging-derived measurement of the volume of the extravascular extracellular space in glioblastoma multiforme. *AJNR Am J Neuroradiol* 2010; 31: 549–53. doi:10.3174/ajnr.A1844.
- [24] Simonetti AJ, Hoogenraad FG, van Muiswinkel AMC. Automated arterial input function using spatial information and feature space reduction. Proceedings of 2007 Annual Scientific Meeting of International Society of Magnetic Resonance in Medicine, abstract number 2820.
- [25] Tofts PS, Brix G, Buckley DL, et al. Estimating kinetic parameters from dynamic contrast-enhanced T1-weighted MRI of a diffusible tracer: standardized quantities and symbols. *J Magn Reson Imaging* 1999; 10: 223–32. doi:10.1002/(SICI)1522-2586(199909)10:3<223::AID-JMRI2>3.0.CO;2-S.
- [26] Langer DL, van der Kwast TH, Evans AJ, Trachtenberg J, Wilson BC, Haider MA. Prostate cancer detection with multiparametric MRI: logistic regression analysis of quantitative T2, diffusion-weighted imaging and dynamic contrast-enhanced MRI. *J Magn Reson Imaging* 2009; 30: 327–34. doi:10.1002/jmri.21824.
- [27] Yankeelov TE, Lepage M, Chakravarthy A, et al. Integration of quantitative DCE-MRI and ADC mapping to monitor treatment response in human breast cancer: initial results. *Magn Reson Imaging* 2007; 25: 1–13. doi:10.1016/j.mri.2006.09.006.
- [28] Wesseling P, Ruitter DJ, Burger PC. Angiogenesis in brain tumors: pathobiological and clinical aspects. *J Neurooncol* 1997; 32: 253–65. doi:10.1023/A:1005746320099.
- [29] Ross BD, Galban CJ, Rehemtulla A, et al. Diffusion and MR imaging in adult neoplasia. In: Gillard JH, Waldman AD, Barker PB, editors. Clinical MR neuroimaging physiological and functional techniques. 2nd ed. New York: Cambridge University Press; 2010, p. 324.
- [30] Riad S, Holodny AI, Mukherji SK. Diffusion imaging in brain tumors and treatment response. In: Holodny AI, editor. Functional neuroimaging: a clinical approach. New York: Informa Healthcare; 2008, p. 204.
- [31] Abo-Ramadan U, Durukan A, Pitkonen M, et al. Post-ischemic leakiness of the blood–brain barrier: a quantitative and systematic assessment by Patlak plots. *Exp Neurol* 2009; 219: 328–33. doi:10.1016/j.expneurol.2009.06.002.
- [32] Sadeghi N, Camby I, Goldman S, et al. Effect of hydrophilic components of the extracellular matrix on quantifiable diffusion-weighted imaging of human gliomas: preliminary results of correlating apparent diffusion coefficient values and hyaluronan expression level. *AJR Am J Roentgenol* 2003; 181: 235–41.